From Planck Data to Planck Era: Observational Tests of Holographic Cosmology

Niayesh Afshordi,[1,2] Claudio Corianò,[3,4,5] Luigi Delle Rose,[3,6,7] Elizabeth Gould,[1,2] and Kostas Skenderis[3,4]
[1]Perimeter Institute for Theoretical Physics, 31 Caroline Street North, Waterloo, Ontario N2L 2Y5, Canada
[2]Department of Physics and Astronomy, University of Waterloo, Waterloo, Ontario N2L 3G1, Canada
[3]STAG Research Centre, Highfield, University of Southampton, SO17 1BJ Southampton, United Kingdom
[4]Mathematical Sciences, Highfield, University of Southampton, SO17 1BJ Southampton, United Kingdom
[5]Dipartimento di Matematica e Fisica "Ennio De Giorgi," Università del Salento and INFN-Lecce, Via Arnesano, 73100 Lecce, Italy
[6]School of Physics and Astronomy, Highfield, University of Southampton, SO17 1BJ Southampton, United Kingdom
[7]Rutherford Appleton Laboratory, Chilton, Didcot OX11 0QX, United Kingdom
(Received 3 August 2016; revised manuscript received 24 October 2016; published 27 January 2017)

We test a class of holographic models for the very early Universe against cosmological observations and find that they are competitive to the standard cold dark matter model with a cosmological constant (ΛCDM) of cosmology. These models are based on three-dimensional perturbative superrenormalizable quantum field theory (QFT), and, while they predict a different power spectrum from the standard power law used in ΛCDM, they still provide an excellent fit to the data (within their regime of validity). By comparing the Bayesian evidence for the models, we find that ΛCDM does a better job globally, while the holographic models provide a (marginally) better fit to the data without very low multipoles (i.e., $l \lesssim 30$), where the QFT becomes nonperturbative. Observations can be used to exclude some QFT models, while we also find models satisfying all phenomenological constraints: The data rule out the dual theory being a Yang-Mills theory coupled to fermions only but allow for a Yang-Mills theory coupled to nonminimal scalars with quartic interactions. Lattice simulations of 3D QFTs can provide nonperturbative predictions for large-angle statistics of the cosmic microwave background and potentially explain its apparent anomalies.

DOI: 10.1103/PhysRevLett.118.041301

Observations of the cosmic microwave background (CMB) offer a unique window into the very early Universe and Planck-scale physics. The standard model of cosmology, the so-called ΛCDM model, provides an excellent fit to the observational data with just six parameters. Four of these parameters describe the composition and evolution of the Universe, while the other two are linked with the physics of the very early Universe. These two parameters, the tilt n_s and the amplitude $\Delta_0^2(q_*)$, parameterize the power spectrum of primordial curvature perturbations,

$$\Delta_{\mathcal{R}}^2(q) = \Delta_0^2(q_*)\left(\frac{q}{q_*}\right)^{n_s-1}, \tag{1}$$

where q_*, the pivot, is an arbitrary reference scale. This form of the power spectrum is a good approximation for slow-roll inflationary models and has the ability to fit the CMB data well. Indeed, a near-power-law scalar power spectrum may be considered as a success of the theory of cosmic inflation.

The theory of inflation is an effective theory. It is based on gravity coupled to (appropriate) matter perturbatively quantized around an accelerating Friedmann-Lemaître-Robertson-Walker (FLRW) background. At sufficiently early times, the curvature of the FLRW spacetime becomes large and the perturbative treatment is expected to break down—in this regime, we would need a full-fledged theory of quantum gravity. One of the deepest insights about quantum gravity that emerged in recent times is that it is expected to be holographic [1–3], meaning that there should be an equivalent description of the bulk physics using a quantum field theory with no gravity in one dimension less. One may thus seek to use holography to model the very early Universe.

Holographic dualities were originally developed for spacetimes with a negative cosmological constant (the AdS/CFT duality) [3], and soon afterwards the extension to de Sitter and cosmology was considered [4–8]. In this context, the statement of the duality is that the partition function of the dual quantum field theory (QFT) computes the wave function of the Universe [8], and using this wave function cosmological observables may be obtained. Alternatively [9–13], one may use the domain-wall–cosmology correspondence [14]. The two approaches are equivalent [15].

Holography offers a new framework that can accommodate conventional inflation but also leads to qualitatively new models for the very early Universe. While conventional inflation corresponds to a strongly coupled QFT [16–32], the new models are associated with a weakly coupled QFT. These models correspond to a nongeometric bulk, and yet holography allows us to compute the predictions for the cosmological observables. We emphasize that the application of holography to cosmology is conjectural, the theoretical validity of such dualities is still open, and different authors approach the topic in different ways. Here we seek to test these ideas against observations.

A class of nongeometric models were introduced in Ref. [9], and their predictions have been worked out in Refs. [9–13,33,34]. These models are based on three-dimensional superrenormalizable QFT, and they universally predict a scalar power spectrum of the form

$$\Delta^2_{\mathcal{R}}(q) = \frac{\Delta_0^2}{1 + (gq_*/q)\ln|q/\beta gq_*| + \mathcal{O}(gq_*/q)^2}, \quad (2)$$

where g is related to the coupling constant of the dual QFT, while β depends on the parameters of the dual QFT (see below).

The form of the power spectrum in (2) is distinctly different from (1). [For small enough g, one may rewrite (2) in the form (1) with momentum-dependent $n_s(q)$. However, as discussed [9,35], the momentum dependence of $n_s(q)$ is qualitatively different from that of slow-roll inflationary models [36].] Since these are qualitatively different parametrizations, one may ask which of the two is preferred by the data. Note that this question is *a priori* independent of the underlying physical models that produced (1) and (2). This question has already been addressed for WMAP7 data [37] in Refs. [35,38], and it was found that, while the data mildly favor ΛCDM, it was insufficient to definitively discriminate between the two cases. Since then, the Planck mission has released its data [39], and it is now time to revisit this issue. We will present the main conclusions of the fit to Planck data here, referring to Ref. [40] for a more detailed discussion.

On the theoretical side, there has also been significant progress since Ref. [35]. While the form of (2) is universally fixed, the precise relation between g and β and the parameters of the dual QFT requires a two-loop computation, which has now been carried out in Ref. [41]. We can thus not only check whether (2) is compatible with CMB data, but also use the data to do a model selection.

Theory.—Following Ref. [9], we consider the dual QFT to be an $SU(N)$ gauge theory coupled to scalars Φ^M and fermions ψ^L, where M and L are flavor indices. The action is given by

$$S = \frac{1}{g^2_{\rm YM}}\int d^3x \mathrm{tr}\left[\frac{1}{2}F_{ij}F^{ij} + (\mathcal{D}\Phi)^2 + 2\overline{\psi}\not{\mathcal{D}}\psi + 2\sqrt{2}\mu(\Phi\overline{\psi}\psi) + \frac{1}{6}\lambda\Phi^4\right], \quad (3)$$

where all fields, $\varphi = \varphi^a T^a$, are in the adjoint of $SU(N)$ and $\mathrm{tr}T^aT^b = \frac{1}{2}\delta^{ab}$. F_{ij} is the Yang-Mills field strength, and $\mathcal{D}$ is a gauge covariant derivative. We use the shorthand notation $(\mathcal{D}\Phi)^2 = \delta_{M_1M_2}\mathcal{D}_i\Phi^{M_1}\mathcal{D}^i\Phi^{M_2}$, $\overline{\psi}\not{\mathcal{D}}\psi = \delta_{L_1L_2}\overline{\psi}^{L_1}\gamma^i\mathcal{D}_i\psi^{L_2}$, $\mu(\Phi\overline{\psi}\psi) \equiv \mu_{ML_1L_2}\Phi^M\overline{\psi}^{L_1}\psi^{L_2}$, and $\lambda\Phi^4 \equiv \lambda_{M_1M_2M_3M_4}\Phi^{M_1}\Phi^{M_2}\Phi^{M_3}\Phi^{M_4}$.

The holographic dictionary relates the scalar and tensor power spectra to the two-point function of the energy-momentum tensor T_{ij}. For the scalar power spectrum,

$$\Delta^2_{\mathcal{R}}(q) = \frac{1}{4\pi^2N^2 f(g^2_{\rm eff})}, \quad (4)$$

where $g^2_{\rm eff}(q) \equiv g^2_{\rm YM}N/q$ is the effective dimensionless 't Hooft coupling constant, q is the magnitude of the momentum $\vec{q}$, and $f(g^2_{\rm eff})$ is extracted from the momentum space two-point function of the trace of the energy-momentum tensor, $\langle T^i_i(\vec{p})T^j_j(\vec{q})\rangle = (2\pi)^3\delta(\vec{p}+\vec{q})q^3N^2 f(g^2_{\rm eff})$. In perturbation theory,

$$f(g^2_{\rm eff}) = f_0[1 - f_1 g^2_{\rm eff}\ln g^2_{\rm eff} + f_2 g^2_{\rm eff} + \mathcal{O}(g^4_{\rm eff})]. \quad (5)$$

The function f_0 is determined by a one-loop computation, while f_1 and f_2 come from two loops. The presence of the logarithm is due to UV and IR divergences in the computation of the two-point function of the energy-momentum tensor. A detailed derivation of (4) may be found in Refs. [10,35]. Following Ref. [35], Eq. (2) and Eqs. (4) and (5) match if

$$gq_* = f_1 g^2_{\rm YM}N, \qquad \ln\frac{1}{\beta} = \frac{f_2}{f_1} + \ln|f_1|,$$
$$\Delta_0^2 = \frac{1}{4\pi^2N^2f_0}. \quad (6)$$

So, a universal prediction of these class of theories is the power spectrum (2), independent of the details of the two-loop computation. [This assumes $f_1 \neq 0$. A separate analysis is required, where $f_1 = 0$, e.g., for (3) without gauge fields and fermions].

The one-loop computation was done in Refs. [9,10], and we here report the result of the two-loop computation [41,42]. The final result is

$$f_0 = \frac{1}{64}\mathcal{N}_{(B)}, \qquad \mathcal{N}_{(B)} = 1 + \sum_M(1-8\xi_M)^2, \quad (7)$$

$$f_1 = -\frac{4}{3\pi^2}\frac{1}{\mathcal{N}_{(B)}}\left(\mathcal{N}_\psi - 2 + 2\mathcal{N}_\Phi + \frac{1}{2}\mu^2 - 48\Sigma_\Phi\right), \quad (8)$$

$$\ln\beta = \ln\frac{1}{|g|} - \frac{a_0}{f_1} - \frac{64/\pi^2}{f_1\mathcal{N}_{(B)}}\Sigma_\Phi\ln\frac{Nf_1}{g}, \quad (9)$$

where $\mathcal{N}_\Phi$ and $\mathcal{N}_\psi$ are the total number of scalars and fermions, respectively, and

$$a_0 = -\frac{1}{24\pi^2 \mathcal{N}_{(B)}}\Big\{16 + 3\pi^2 - 56\mathcal{N}_\psi - 4\sum_M \mu^2_{MM} + \sum_M 3(8\xi_M - 1) \times [8(\pi^2 - 16)\xi_M - 3\pi^2 + 112 + 2\mu^2_{MM}] + \pi^2 \sum_{M_1,M_2} \lambda_{M_1M_1M_2M_2}(8\xi_{M_1} - 1)(8\xi_{M_2} - 1)\Big\},$$

$$\Sigma_\Phi = \sum_M \xi_M^2 \left(2 + \frac{1}{2}\mu^2_{MM}\right),$$

where $\mu^2_{M_1M_2} = \sum_{L_1,L_2} \mu_{M_1L_1L_2}\mu_{M_2L_2L_1}$, ξ_M is the nonminimality parameter, and summations over $M(L)$ are over scalars (fermions). [Nonminimal scalars on a curved background have the coupling $1/(2g^2_{\rm YM})\sum_M \int \xi_M R(\Phi^M)^2$, where R is the curvature scalar, and this term induces an "improvement term" to their energy-momentum tensor, $T_{ij} = (2/\sqrt{g})(\delta S/\delta g^{ij})|_{g_{ij}=\delta_{ij}}$; see [42]].

Fitting to the data.—We would like now to assess how well a power spectrum of the form (2) fits the cosmological data and compare with that of the conventional power-law power spectrum. Recall that ΛCDM is parametrized by six parameters $(\Omega_b h^2, \Omega_c h^2, \theta, \tau, \Delta_0^2, n_s)$, where $\Omega_b h^2$ and $\Omega_c h^2$ are the baryon and dark matter densities, respectively, θ is the angular size of the sound horizon at recombination, τ is the optical depth due to reionization, and Δ_0^2 and n_s are the parameters entering in (1). To formalize the comparison, we define (following Ref. [35]) holographic cosmology (HC) as the model parametrized by $(\Omega_b h^2, \Omega_c h^2, \theta, \tau, \Delta_0^2, g, \ln\beta)$. (In Ref. [35], the parameter β was incorrectly assumed to be equal to one. We refitted the WMAP data and found that the global minimum is at $\beta = 3.777$.) This model has seven parameters, so, in order to compare models with the same number of parameters, we also consider ΛCDM with running $\alpha_s = dn_s/d\ln q$. Note that our aim here is to compare *empirical models*, not the underlying physical models that lead to them. If the data select one of the two empirical models, then this would falsify all physical models that underlie the other model.

We analyzed the data using CosmoMC [47–53]. We ran both ΛCDM and HC with the same data sets, fitting the models to the Planck 2015 data including lensing [39,54–59], as well as baryonic acoustic oscillations (BAO) [60–67] and BICEP2-Keck-Planck (BKP) polarization [68]. After CosmoMC had run to determine the mean and errors in the parameters, we ran the minimizer [69] within the code to determine the best fit parameters and likelihood.

The Planck angular TT spectrum together with the best fit curves and residuals for HC and ΛCDM are presented in Fig. 1. Notice that the difference between ΛCDM and HC lies within the 68% region of Planck, with the largest difference being at small multipoles. Very similar results hold for the TE and EE spectra [40]. We determined the best fit values for all parameters for HC, ΛCDM, and ΛCDM with running. Our values for the parameters of ΛCDM and ΛCDM with running are in agreement with those determined by the Planck team. All common parameters of the three models are within 1σ of each other (with the notable exception of the optical depth τ [40]). We report the values of Δ_0, g, $\ln\beta$, and χ^2 in Table I (the list of all parameters can be found in Ref. [40]). The χ^2 of the fit indicates that HC is disfavored at about 2.2σ relative to ΛCDM with running, when we consider all multipoles.

Relative to the WMAP fit in Ref. [35], the value of g has decreased from -1.3×10^{-3} to -7×10^{-3}. In Fig. 2, we investigate how the value of g changes if we change the range of multipoles that we consider. It is clear from the plot that the value of g is compatible between WMAP and Planck, if we keep the same multipoles. It is also clear that the high l modes want to push g to lower negative values.

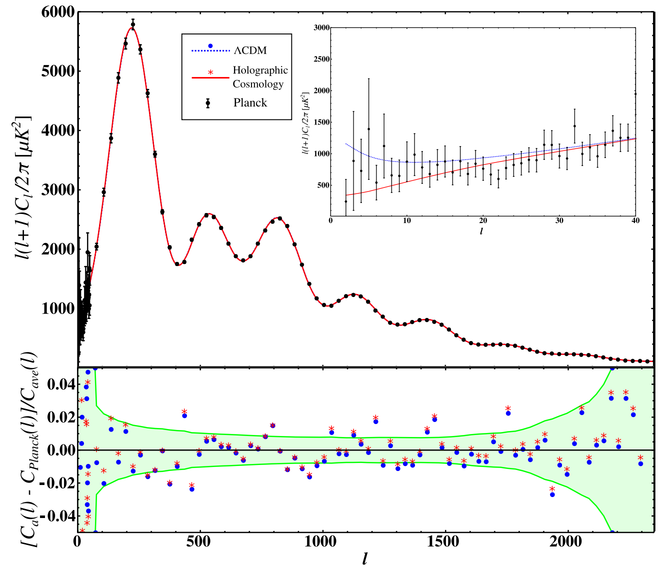

FIG. 1. Angular power spectrum of CMB temperature anisotropies, comparing Planck 2015 data with best fit ΛCDM (dotted blue curve) and holographic cosmology (solid red curve) models, for $l \geq 30$. The lower panel shows the relative residuals, where the green shaded region indicates the 68% region of Planck 2015 data.

TABLE I. Upper part: Planck 2015 + BAO + BKP mean parameters for holographic cosmology. Lower part: χ^2 values for a fit with all multipoles and a fit with $l < 30$ multipoles excluded.

HC	$10^9 \Delta_0^2$	g	$\ln\beta$
All l	$2.126^{+0.058}_{-0.058}$	$-0.00703^{+0.00105}_{-0.00167}$	$0.877^{+0.186}_{-0.239}$
$l \geq 30$	$2.044^{+0.072}_{-0.075}$	$-0.01305^{+0.00452}_{-0.00345}$	$1.014^{+0.206}_{-0.272}$
	HC	ΛCDM	ΛCDM running
χ^2 (all l)	11324.5	11319.9	11319.6
$\chi^2(l \geq 30)$	824.0	824.5	823.5

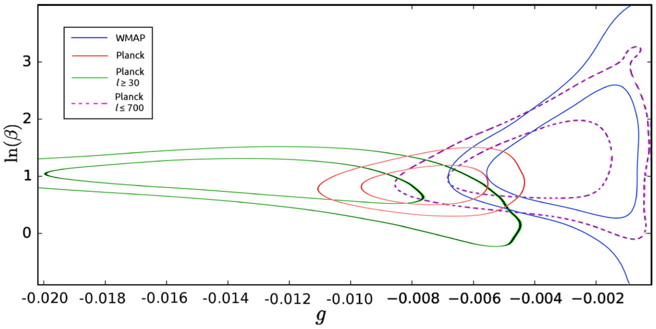

FIG. 2. Plot of 1σ and 2σ regions in parameter space for holographic cosmology g and $\ln(\beta)$ values for WMAP (blue line, right), Planck (red line, middle), Planck with $l < 30$ values removed (green line, left), and Planck with $l > 700$ values ignored (purple dashed line). We see that higher resolution data progressively push g to lower negative values.

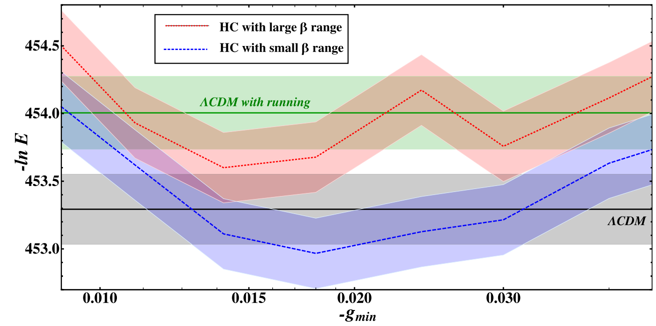

FIG. 3. Bayesian evidence using $l \geq 30$ data only, where the perturbative expansion (2) can be trusted. An error is indicated by the shaded region around the lines.

Larger values of $|g|$ indicate that the theory may become nonperturbative at very low l, and, as such, the predictions of the model cannot be trusted in that regime. We shall see below that this is supported by model selection criteria. Therefore, we repeat the fitting, excluding the $l < 30$ multipoles. The results for Δ_0, g, $\ln\beta$, and χ^2 are tabulated in Table I. With these data, all common parameters are now compatible with each other [40]. The χ^2 test shows that the three models are now within 1σ.

The power spectrum for the tensors takes the same form as (2) but with different values of g and β. We fitted the data with this form of the power spectrum and found that it is consistent with $r = 0$; the 2σ upper limit on the tensor-to-scalar ratio is $r < 0.125$.

Bayesian evidence.—In comparing different models, one often uses information criteria such as the value of χ^2, which quantifies the goodness of a fit. We emphasize that with "model" we mean the three empirical models introduced above: ΛCDM, ΛCDM with running, and HC. What we really want to know, however, is what the probability is for each of these models given the data. This is obtained by computing the Bayesian evidence.

As discussed in Ref. [35], if we assume flat priors for all parameters α_M that define a given model, the Bayesian evidence is given by $E = (1/\mathrm{Vol}_M)\int d\alpha_M \mathcal{L}(\alpha_\mathcal{M})$, where $\mathcal{L}(\alpha_\mathcal{M})$ is the likelihood and Vol_M is the volume of the region in parameter space over which the prior probability distribution is nonzero. The evidence may be computed either by using CosmoMC or by MultiNest [70–72].

Note that the aim here is to compare empirical models, and we determined the priors from previous fits of the same empirical models to the data (as is common). (Had we focused on specific physical models, we could use the wave function of the Universe to obtain corresponding theoretical priors; see [18] for work in this direction.) We use the priors in Table 4 of Ref. [35], except that the upper limit of 100θ is taken to be 1.05. The prior for the running is taken to be $|\alpha_s| \leq 0.05$. The priors for n_s are the asymmetric prior used in Ref. [35]: $0.92 \leq n_s \leq 1$. For the prior for g, we use a variable range, $g_{\rm min} \leq g < 0$. This prior is fixed by the requirement that the perturbation theory is valid. We will allow for the possibility that the perturbative expansion is valid only for $l > 30$. We use as a rough estimate for the validity of perturbation theory that gq^*/q is sufficiently small, taking this to mean a value between 0.20 and 1 at $l = 30$. (The momenta and multipoles are related via $q = l/r_h$, where $r_h = 14.2$ Gpc is the comoving radius of the last scattering surface.) This translates into $-0.009 < g_{\rm min} < -0.45$. The prior for β is fixed by using the results from (our fit to) WMAP data. We use two sets of priors: one coming from the 1σ range ($0 \leq \ln\beta \leq 2$) and the other from the 2σ range ($-0.2 \leq \ln\beta \leq 3.5$).

The results for the Bayesian evidence are presented in Fig. 3 for $l \geq 30$, where two-loop predictions (2) can be trusted. As a guide [73], a difference $\ln E < 1$ is insignificant and $2.5 < \ln E < 5$ is strongly significant. We see that the difference between evidence for ΛCDM and HC predictions is insignificant, with marginal preference for HC, depending on the choice of priors.

Model selection.—We would like now to examine whether we can use the data to rule out or in some of the models described by (3). There are phenomenological and theoretical constraints that we need to satisfy. The phenomenological constraints are that the bound on the tensor-to-scalar ratio $r \leq 0.125$ should be satisfied and the model should reproduce the observed values for the amplitude Δ_0^2 and $\ln\beta$. The theoretical prediction for the r is [9,10,34]

$$r = 32\frac{1 + \sum_{M=1}^{\mathcal{N}_\Phi}(1 - 8\xi_M)^2}{1 + 2\mathcal{N}_\psi + \mathcal{N}_\Phi}, \tag{10}$$

and the theoretical predictions for Δ_0^2 and $\ln\beta$ are given in (6)–(9). In deriving (2), we used a 't Hooft large N expansion and perturbation theory in $g_{\rm eff}^2$. We thus need to check that any solution of the phenomenological constraints is consistent with these theoretical assumptions.

There are a few universal properties of the two-loop correction $gq_*/q \ln|q/\beta g q_*|$. This term vanishes at large q, reflecting the fact that the QFTs we consider are super-renormalizable. Its absolute value gradually increases till it reaches the local maximum $1/e\beta$ at $q = e\beta|g|q_*$. At lower values of l, the two-loop term changes sign and grows very fast as we go to lower multipoles becoming equal to one (same size as the one-loop contribution) below $l = 10$. Therefore, we should not trust these models below $l \sim 10$. In fact, one should even be cautious in using the two-loop approximation for l's lower than 35. While the overall magnitude of the two-loop term is small up until $l = 10$, this happens due to a large cancellation between the f_1 and the f_2 term in (5). We will use as an indicator of the reliability of perturbation theory the size of $f_1 g_{\rm eff}^2 \ln g_{\rm eff}^2$.

Let us consider a gauge theory coupled to a large number $\mathcal{N}_\Phi$ of nonminimal scalars, all with the same nonminimality parameter ξ and the same quartic coupling λ. For sufficiently large $\mathcal{N}_\Phi$, the scalar-to-tensor ratio (10) becomes

$$r = 32(1 - 8\xi)^2, \tag{11}$$

and the bound on r implies $|1 - 8\xi| \leq 0.061$, where the equality holds when $r = 0.12$. Choosing a value of ξ, then the observational values of Δ_0^2 and $\ln\beta$ give two equations, which can always be solved to determine N and $\mathcal{N}_\Phi$. For example, if we choose $\xi = 0.133$, which corresponds to $r = 0.12$, and take $\lambda = 1$, the solution to the two constraints is

$$N = 2995, \qquad \mathcal{N}_\Phi = 23255. \tag{12}$$

This solution satisfies the theoretical constraints: First, $N^2 \gg \mathcal{N}_\Phi$, so the large N expansion is justified and, second, the effective coupling remains small for all momenta seen by Planck, $3.3 \times 10^{-4} \leq g_{\rm eff}^2(q) \leq 0.41$. For this solution, however, $f_1 \approx -8(1 - 48\xi^2)/(1 - 8\xi)^2 \approx -11$ and $f_1 g_{\rm eff}^2 \ln g_{\rm eff}^2 \approx 1$ when $l = 35$, so we should not trust the perturbative expansion below around $l \approx 35$.

Conclusions.—We showed that holographic models based on three-dimensional perturbative QFT are capable of explaining the CMB data and are competitive to the ΛCDM model. However, at very low multipoles (roughly $l < 30$), the perturbative expansion breaks down, and in this regime the prediction of the theory cannot be trusted. The data are consistent with the dual theory being a gauge theory coupled to a large number of nearly conformal scalars with a quartic interaction. It would be interesting to further analyze these models in order to extract other properties that may be testable against observations. In particular, nonperturbative methods (such as putting the dual QFT on a lattice) can be used to reliably model the very low multipoles, which may potentially explain the apparent large-angle anomalies in the CMB sky (e.g., [74]).

We thank Raphael Flauger for collaboration at early stages of this work. K. S. is supported in part by the Science and Technology Facilities Council (Consolidated Grant "Exploring the Limits of the Standard Model and Beyond"). K. S. thanks GGI in Florence for hospitality during the final stages of this work. N. A. and E. G. were supported in part by Perimeter Institute for Theoretical Physics. Research at Perimeter Institute is supported by the Government of Canada through the Department of Innovation, Science and Economic Development Canada and by the Province of Ontario through the Ministry of Research, Innovation and Science. We acknowledge the use of the Legacy Archive for Microwave Background Data Analysis (LAMBDA), part of the High Energy Astrophysics Science Archive Center (HEASARC). HEASARC/LAMBDA is a service of the Astrophysics Science Division at the NASA Goddard Space Flight Center. L. D. R. is partially supported by the "Angelo Della Riccia" foundation. The work of C. C. was supported in part by *The Leverhulme Trust Visiting Professorship* at the STAG Research Centre and Mathematical Sciences, University of Southampton.

[1] G. 't Hooft, in *Proceedings of the Conference on Highlights of Particle and Condensed Matter Physics (Salamfest), Trieste, Italy, 1993* (World Scientific, Singapore, 1993), pp. 284–296.
[2] L. Susskind, J. Math. Phys. (N.Y.) **36**, 6377 (1995).
[3] J. M. Maldacena, Int. J. Theor. Phys. **38**, 1113 (1999); Adv. Theor. Math. Phys. **2**, 231 (1998).
[4] C. M. Hull, J. High Energy Phys. 07 (1998) 021.
[5] E. Witten, arXiv:hep-th/0106109.
[6] A. Strominger, J. High Energy Phys. 10 (2001) 034.
[7] A. Strominger, J. High Energy Phys. 11 (2001) 049.
[8] J. M. Maldacena, J. High Energy Phys. 05 (2003) 013.
[9] P. McFadden and K. Skenderis, Phys. Rev. D **81**, 021301 (2010).
[10] P. McFadden and K. Skenderis, J. Phys. Conf. Ser. **222**, 012007 (2010).
[11] P. McFadden and K. Skenderis, J. Cosmol. Astropart. Phys. 05 (2011) 013.
[12] P. McFadden and K. Skenderis, J. Cosmol. Astropart. Phys. 06 (2011) 030.
[13] A. Bzowski, P. McFadden, and K. Skenderis, J. High Energy Phys. 03 (2012) 091.
[14] K. Skenderis and P. K. Townsend, Phys. Rev. Lett. **96**, 191301 (2006).
[15] J. Garriga, K. Skenderis, and Y. Urakawa, J. Cosmol. Astropart. Phys. 01 (2015) 028.
[16] J. M. Maldacena and G. L. Pimentel, J. High Energy Phys. 09 (2011) 045.
[17] J. B. Hartle, S. W. Hawking, and T. Hertog, arXiv: 1205.3807.
[18] J. B. Hartle, S. W. Hawking, and T. Hertog, J. Cosmol. Astropart. Phys. 01 (2014) 015.
[19] K. Schalm, G. Shiu, and T. van der Aalst, J. Cosmol. Astropart. Phys. 03 (2013) 005.

[20] A. Bzowski, P. McFadden, and K. Skenderis, J. High Energy Phys. 04 (2013) 047.
[21] I. Mata, S. Raju, and S. Trivedi, J. High Energy Phys. 07 (2013) 015.
[22] J. Garriga and Y. Urakawa, J. Cosmol. Astropart. Phys. 07 (2013) 033.
[23] P. McFadden, J. High Energy Phys. 10 (2013) 071.
[24] A. Ghosh, N. Kundu, S. Raju, and S. P. Trivedi, J. High Energy Phys. 07 (2014) 011.
[25] J. Garriga and Y. Urakawa, J. High Energy Phys. 06 (2014) 086.
[26] N. Kundu, A. Shukla, and S. P. Trivedi, J. High Energy Phys. 04 (2015) 061.
[27] P. McFadden, J. High Energy Phys. 02 (2015) 053.
[28] N. Arkani-Hamed and J. Maldacena, arXiv:1503.08043.
[29] N. Kundu, A. Shukla, and S. P. Trivedi, J. High Energy Phys. 01 (2016) 046.
[30] T. Hertog and E. van der Woerd, J. Cosmol. Astropart. Phys. 02 (2016) 010.
[31] J. Garriga, Y. Urakawa, and F. Vernizzi, J. Cosmol. Astropart. Phys. 02 (2016) 036.
[32] J. Garriga and Y. Urakawa, J. Cosmol. Astropart. Phys. 10 (2016) 030.
[33] C. Corianò, L. Delle Rose, and M. Serino, J. High Energy Phys. 12 (2012) 090.
[34] S. Kawai and Y. Nakayama, J. High Energy Phys. 06 (2014) 052.
[35] R. Easther, R. Flauger, P. McFadden, and K. Skenderis, J. Cosmol. Astropart. Phys. 09 (2011) 030.
[36] A. Kosowsky and M. S. Turner, Phys. Rev. D **52**, R1739 (1995).
[37] E. Komatsu *et al.* (WMAP Collaboration), Astrophys. J. Suppl. Ser. **192**, 18 (2011).
[38] M. Dias, Phys. Rev. D **84**, 023512 (2011).
[39] P. A. R. Ade *et al.* (Planck Collaboration), Astron. Astrophys. **594**, A13 (2016).
[40] N. Afshordi, E. Gould, and K. Skenderis (to be published).
[41] C. Corianò, L. Delle Rose, and K. Skenderis (to be published).
[42] See Supplemental Material at http://link.aps.org/supplemental/10.1103/PhysRevLett.118.041301 for technical details, which includes Refs. [43–46].
[43] A. Jevicki, Y. Kazama, and T. Yoneya, Phys. Rev. D **59**, 066001 (1999).
[44] I. Kanitscheider, K. Skenderis, and M. Taylor, J. High Energy Phys. 09 (2008) 094.
[45] R. Jackiw and S. Templeton, Phys. Rev. D **23**, 2291 (1981).
[46] T. Appelquist and R. D. Pisarski, Phys. Rev. D **23**, 2305 (1981).
[47] U. Seljak and M. Zaldarriaga, Astrophys. J. **469**, 437 (1996).
[48] M. Zaldarriaga, U. Seljak, and E. Bertschinger, Astrophys. J. **494**, 491 (1998).
[49] A. Lewis, A. Challinor, and A. Lasenby, Astrophys. J. **538**, 473 (2000).
[50] A. Lewis and S. Bridle, Phys. Rev. D **66**, 103511 (2002).
[51] C. Howlett, A. Lewis, A. Hall, and A. Challinor, J. Cosmol. Astropart. Phys. 04 (2012) 027.
[52] A. Lewis, Phys. Rev. D **87**, 103529 (2013).
[53] A. Lewis, CAMB Notes, http://cosmologist.info/notes/CAMB.pdf.
[54] P. Ade *et al.* (Planck Collaboration), Astron. Astrophys. **594**, A15 (2016).
[55] N. Aghanim *et al.* (Planck Collaboration), Astron. Astrophys. **594**, A11 (2016).
[56] P. Ade *et al.* (Planck Collaboration), Astron. Astrophys. **594**, A24 (2016).
[57] C. Bennett *et al.* (WMAP Collaboration), Astrophys. J. Suppl. Ser. **208**, 20 (2013).
[58] C. Reichardt *et al.*, Astrophys. J. **755**, 70 (2012).
[59] S. Das *et al.*, J. Cosmol. Astropart. Phys. 04 (2014) 014.
[60] F. Beutler, C. Blake, M. Colless, D. Heath Jones, L. Staveley-Smith, L. Campbell, Q. Parker, W. Saunders, and F. Watson, Mon. Not. R. Astron. Soc. **416**, 3017 (2011).
[61] C. Blake *et al.*, Mon. Not. R. Astron. Soc. **418**, 1707 (2011).
[62] L. Anderson *et al.*, Mon. Not. R. Astron. Soc. **427**, 3435 (2012).
[63] F. Beutler, C. Blake, M. Colless, D. Heath Jones, L. Staveley-Smith, G. B. Poole, L. Campbell, Q. Parker, W. Saunders, and F. Watson, Mon. Not. R. Astron. Soc. **423**, 3430 (2012).
[64] N. Padmanabhan, X. Xu, D. J. Eisenstein, R. Scalzo, A. J. Cuesta, K. T. Mehta, and E. Kazin, Mon. Not. R. Astron. Soc. **427**, 2132 (2012).
[65] L. Anderson *et al.* (BOSS Collaboration), Mon. Not. R. Astron. Soc. **441**, 24 (2014).
[66] L. Samushia *et al.*, Mon. Not. R. Astron. Soc. **439**, 3504 (2014).
[67] A. J. Ross, L. Samushia, C. Howlett, W. J. Percival, A. Burden, and M. Manera, Mon. Not. R. Astron. Soc. **449**, 835 (2015).
[68] P. Ade *et al.*(BICEP2, Planck Collaboration), Phys. Rev. Lett. **114**, 101301 (2015).
[69] M. Powell, The BOBYQA algorithm for bound constrained optimization without derivatives, http://www.damtp.cam.ac.uk/user/na/NA_papers/NA2009_06.pdf.
[70] F. Feroz and M. P. Hobson, Mon. Not. R. Astron. Soc. **384**, 449 (2008).
[71] F. Feroz, M. P. Hobson, and M. Bridges, Mon. Not. R. Astron. Soc. **398**, 1601 (2009).
[72] F. Feroz, M. P. Hobson, E. Cameron, and A. N. Pettitt, arXiv:1306.2144.
[73] R. Trotta, Contemp. Phys. **49**, 71 (2008).
[74] P. A. R. Ade *et al.* (Planck Collaboration), Astron. Astrophys. **571**, A23 (2014).